

## Transport properties of incipient gels

Sune Nørhøj Jespersen\* and Michael Plischke†

*Department of Physics, Simon Fraser University, Burnaby, British Columbia, Canada V5A 1S6*

(Received 21 May 2003; published 13 August 2003)

We investigate the behavior of the shear viscosity  $\eta(p)$  and the mass-dependent diffusion coefficient  $D(m,p)$  in the context of a simple model that, as the cross link density  $p$  is increased, undergoes a continuous transition from a fluid to a gel. The shear viscosity diverges at the gel point according to  $\eta(p) \sim (p_c - p)^{-s}$  with  $s \approx 0.65$ . The diffusion constant shows a remarkable dependence on the mass of the clusters:  $D(m,p) \sim m^{-0.69}$ , not only at  $p_c$  but well into the liquid phase. We also find that the Stokes-Einstein relation  $D\eta \propto k_B T$  breaks down already quite far from the gel point.

DOI: 10.1103/PhysRevE.68.021403

PACS number(s): 82.70.Gg, 61.43.Hv, 36.40.Sx

### I. INTRODUCTION

When a system of polyfunctional molecules is cross linked, the transport properties such as the shear viscosity and the diffusivity can be dramatically affected. In particular, the diffusivity decreases as the number of cross links is increased and the shear modulus increases, diverging at the critical point at which a gel is formed. The diffusivity remains finite as the system gels since monomers and small clusters can diffuse through the tenuous structure that characterizes the amorphous solid close to the critical point. Although gels have been studied for many years [1], their critical behavior remains poorly understood. In particular the question of whether or not there exist universality classes into which different materials can be grouped remains largely unanswered.

In this paper, we report on extensive molecular dynamics simulations of a simple model for a gel. We study the system on the fluid side of the gel point from the simple liquid limit into the critical region. We investigate the structural properties of clusters and calculate both the shear viscosity  $\eta(p)$  and the mass-dependent diffusion constant  $D(m,p)$  as functions of the cross link density  $p$ . We find that as  $p \rightarrow p_c$ ,  $\eta(p) \sim (p_c - p)^{-s}$  with  $s \approx 0.65$ , a value somewhat smaller than that conjectured by de Gennes [2] on the basis of an analogy with a random superconductor network and also predicted recently by Broderix *et al.* [3] for a Rouse-like model network. The mass-dependent diffusion constant  $D(m,p) \sim m^{-0.69}$  for a range of  $p$  near the critical point and  $3 \leq m \leq 50$ . This behavior is consistent with earlier results for  $p = p_c$  [4] and rather close to a prediction [2] made on the basis of a simple scaling argument. On the other hand, our value for this exponent is somewhat larger than the ones found by Küntzel *et al.* in a recent paper [5] in which the exponent varies between 0.5 and 0.25 as the strength of the Zimm hydrodynamic interaction is varied. The diffusion coefficient  $D(m,p) \rightarrow \text{const}$  as  $p \rightarrow p_c$  for  $m$  at least as large as 10 but displays critical behavior in the next leading term. It is also worth noting that, in contrast to simple liquids, the product  $D(p)\eta(p)$  is not a constant but rather reflects the

divergence of  $\eta$  at the gel point.

The structure of this paper is as follows. In Sec. II, we describe our model and the computational details. Section III contains a discussion of the geometric properties of the clusters and the nature of the percolation transition. The shear viscosity calculation and results are described in Sec. IV, and results for the diffusion constants are found in Sec. V. We conclude with a short discussion in Sec. VI.

### II. MODEL

The model is similar to the one employed in Ref. [4], but we include the details below for completeness. Our system is composed of  $N = L^3$  ( $L = 10, 13, 15, 20$ , and 30) particles interacting pairwise through the shifted Lennard-Jones potential

$$U(\mathbf{r}) = \begin{cases} U_{LJ}(r) - U_{LJ}(2.5\sigma), & r \leq 2.5\sigma, \\ 0, & \text{otherwise,} \end{cases} \quad (1)$$

where  $U_{LJ}(r) = 4\epsilon[(\sigma/r)^{12} - (\sigma/r)^6]$ . All of our simulations are three-dimensional (3D) constant energy molecular dynamics simulations corresponding to an average temperature of  $k_B T / \epsilon \approx 1$  and density  $\Phi = 0.8\sigma^{-3}$ . These choices ensure that the system is in the liquid-phase region of the phase diagram [6,7]. We use periodic boundary conditions and a time step of magnitude  $dt = 0.005\tau$ , where  $\tau = \sqrt{m\sigma^2/\epsilon}$  is the reduced Lennard-Jones time. From a typical equilibrium state of this liquid, we let the particles form a specified number  $n$  of permanent chemical bonds if they come closer than  $r_c = 2^{1/6}\sigma \approx 1.12$ , coinciding with the minimum of  $U(r)$ . The bond interaction is a harmonic oscillator potential  $U_{\text{harm}}(r) = 1/2kr^2$ ; in our simulations we take  $k\sigma^2/\epsilon = 2.0$  (different from Ref. [4]). Note that this way of adding bonds violates energy conservation; indeed we actually pump energy into the system when adding bonds. To compensate we cool down the system again after having established the required number of bonds. With this bonding procedure cross linking is very fast—the average distance between the particles is comparable to  $r_c$ , so a large number of particles are available for bonding at any given instant. Each particle can bond to a maximum of  $f = 6$  other particles (excluding itself), and the cross link density  $p$  is then given in terms of the number of bonds  $n$  as  $p = 2n/fN$ . Any number of particles, if fulfil-

\*Email address: sune@mr.au.dk

†Email address: plischke@sfu.ca

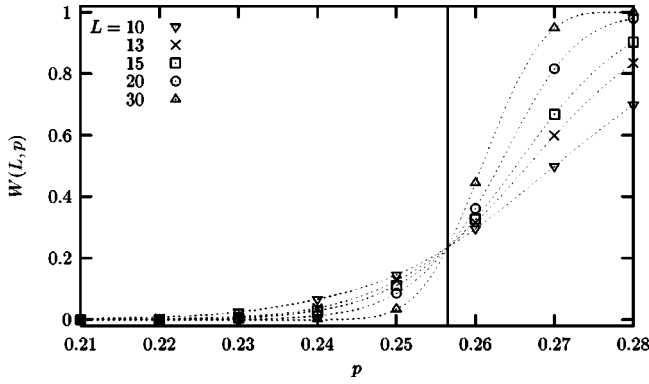


FIG. 1. Fraction of systems,  $W(L,p)$ , percolating in the  $x$  direction as a function of  $p$  for five different system sizes as indicated on the plot. The lines are guides for the eye, except in the case  $L=30$  for which the data are fitted to a stretched exponential [11]. We estimate  $p_c=0.2565$ .

ing the conditions above, can be cross linked per time step, but we halt the bond formation when  $p$  reaches a predetermined value.

### III. GEOMETRIC PROPERTIES

Before discussing the dynamic properties of this model, we need some basic information about the static properties. In this section, we determine the geometrical percolation point  $p_c$  as well as the two critical exponents  $\nu$ , the correlation length exponent, and  $\gamma$ , the exponent characterizing the divergence of the weight average cluster mass (of finite clusters). We follow a procedure similar to the one used and outlined in Refs. [4,8,9]. In order to find  $p_c$ , we calculate numerically the fraction  $W(L,p)$  of percolating systems of size  $L^3$  with a bond density  $p$ . This function is plotted in Fig. 1 for all five system sizes. The crossing points of the different curves seem to coincide, and the corresponding value of  $p$  is thus a good estimate of  $p_c$  [4,10]. From the figure, we determine  $p_c=0.2565$  as in Ref. [4]. Finite size scaling theory predicts that  $W(L,p)$  does not depend on  $L$  and  $p$  separately but only on the combination  $L/\xi$  (and the sign of  $p-p_c$ ), where  $\xi=|p-p_c|^{-\nu}$  is the correlation length and  $\nu$  is the correlation length exponent [12]. Thus we may write

$$W(L,p)=f(L^{1/\nu}(p-p_c)), \quad (2)$$

where  $f(x)$  is a scaling function. To test this hypothesis, we replot the data for  $W(L,p)$  from Fig. 1 in Fig. 2 as a function of  $L^{1/\nu}(p-p_c)$  with  $p_c=0.2565$  as determined above and  $\nu=0.9$ . The collapse is very good, confirming the correctness of the values for  $p_c$  and  $\nu$ .

To compare with percolation theory we need one more exponent, and here we consider the behavior of the weight average cluster mass  $M_w$ . In the thermodynamic limit, the expected behavior is  $M_w(p) \sim |p-p_c|^{-\gamma}$  [12]. Therefore we compute  $M_w$  as a function of  $p$  for different system sizes, and in Fig. 3 we plot the results in the form  $M_w/L^{\gamma/\nu}$  versus

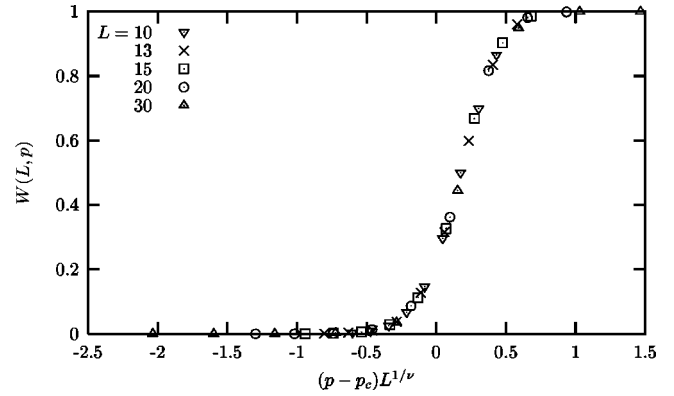


FIG. 2. Same as Fig. 1, except here  $W(L,p)$  is plotted as a function of  $L^{1/\nu}(p-p_c)$  with  $p_c=0.2565$  and  $\nu=0.9$ . The data collapse very nicely in agreement with finite size scaling theory.

$L^{1/\nu}(p_c-p)$  with  $\gamma=1.8$  being the expected 3D percolation value and  $\nu$  and  $p_c$  as determined previously. Again there is a very nice data collapse, and we therefore conclude that here as in Refs. [4,8,9] our system is consistent with the 3D percolation universality class insofar as static properties are concerned.

### IV. VISCOSITY

We measure the shear viscosity  $\eta(p)$  by using the appropriate Green-Kubo formula [13,14]:

$$\eta = \frac{1}{Vk_B T} \int_0^\infty dt \langle \sigma_{xy}(t) \sigma_{xy}(0) \rangle, \quad (3)$$

where  $V$  is the volume and  $\sigma_{xy}(t)$  is the  $xy$  component of the stress tensor:

$$\sigma_{xy}(t) = \sum_{i=1}^N m v_{x,i} v_{y,i} + \sum_{i=1}^N \sum_{j<i} (y_i - y_j) f_{x,ij}. \quad (4)$$

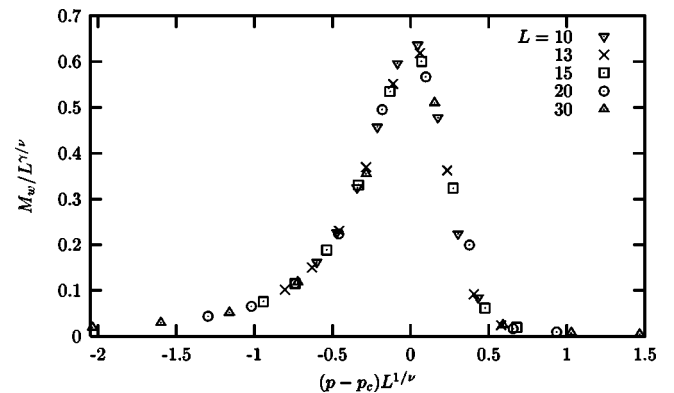


FIG. 3. Scaling plot of the weight average molecular weight  $M_w$ . The quality of the data collapse confirms  $\gamma=1.8$  in accordance with the 3D percolation value.

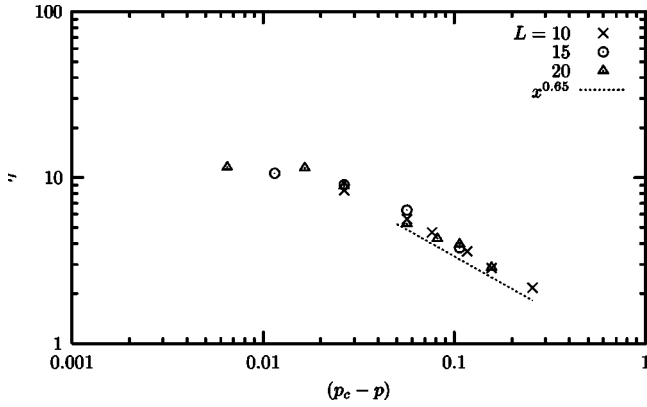


FIG. 4. The dimensionless shear viscosity as a function of  $p_c - p$  for different  $L$ .

In this equation,  $f_{x,ij}$  is the  $x$  component of the force from particle  $j$  on particle  $i$ , and the meaning of the remaining terms is self-explanatory. In the simulations, we average over several hundred samples for each  $p$  and over three off-diagonal components ( $xy, yz$ , and  $zx$ ) of the stress tensor to obtain slightly better statistics. It is important to note that we have discarded any sample containing a spanning cluster since for such a system the viscosity is not defined, i.e., the right hand side of Eq. (3) diverges. Although we have simulated very long runs (up to  $t=750\tau$ ), the stress correlator  $C_{\sigma\sigma}(t) \equiv \langle \sigma_{xy}(t) \sigma_{xy}(0) \rangle$  has still not decayed completely and it is necessary to add by hand an additional contribution, in particular for  $p$  close to  $p_c$ . A stretched exponential  $C_{\sigma\sigma}(t) = a \exp(-bt^c)$  with  $0.1 < c < 0.3$  seems to fit the data well for long times, and there are also theoretical reasons [15] to believe that this is the appropriate form. See Ref. [9] for a thorough discussion of this point.

In Fig. 4, we have plotted the resulting values for the viscosity for different systems sizes and at different stages of the cross linking. We note the clear power-law behavior outside the critical region, and a fit to the  $L=10$  data in this region yields  $s=0.65$ . The line  $\eta \propto (p_c - p)^{-0.65}$  has also been drawn on the plot, and it is apparent that the data are consistent with this exponent. For large  $p$ ,  $p > 0.23$ , there are larger error bars and this will also affect the scaling plot. Since the viscosity diverges at the critical point with an exponent  $s > 0$ , the finite size scaling form is

$$\eta(p, L) = L^{-s/\nu} g(\xi/L), \quad p < p_c, \quad (5)$$

where  $g$  is a scaling function with the limits

$$g(x) \propto \begin{cases} x^{-s/\nu}, & x \rightarrow 0, \\ \text{const}, & x \rightarrow \infty, \end{cases} \quad (6)$$

and  $\xi \sim (p_c - p)^{-\nu}$  is the correlation length, cf. Sec. III. Therefore we plot in Fig. 5  $\eta L^{s/\nu}$  versus  $L^{1/\nu}(p_c - p)$  and the collapse is quite good outside the critical region with  $s = 0.65$ , whereas there is a larger scattering of the points for  $p$  closer to  $p_c$ .

de Gennes has suggested [2] a value of  $s \approx 0.7$  based on an analogy between gelation and conductance in a random

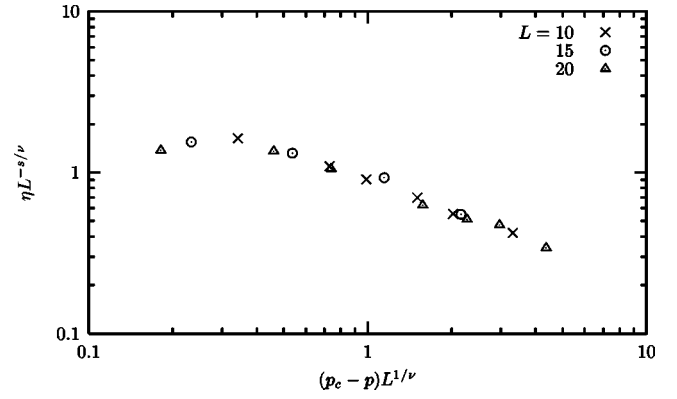


FIG. 5. Same as Fig. 4, but here plotted in a scaling form with  $s=0.65$ .

mixture of normal and superconducting elements, and a good agreement with this was found in a related model in Ref. [9]. Here we have observed a slightly smaller value for  $s$ .

## V. DIFFUSION

In this section, we extend our earlier study [4] on the diffusion of clusters. Previously, we were concerned mainly with the behavior of the diffusion constant  $D(m, p)$  as a function of cluster mass  $m$  at the gelation point  $p = p_c$ . Here we address the  $p$  dependence of  $D$  for different clusters and the validity of the Stokes-Einstein relation  $D(p) \propto k_B T / \eta(p)$  for a given cluster mass. We restrict our attention to the  $L=20$  system.

To determine the diffusion constant, we use the Einstein relation:

$$\frac{1}{6t} \langle (r_m(t) - r_m(0))^2 \rangle \xrightarrow{t \rightarrow \infty} D(m, p), \quad (7)$$

where  $r_m(t)$  is the center-of-mass position of a cluster of mass  $m$  at time  $t$ , for a given value of  $p$  (for clarity of the presentation, we omit the explicit dependence on  $p$  in the notation). When calculating the diffusion constant numerically we have averaged over all clusters of a given mass  $m$  and over several hundred cross linkings, and we have discarded any percolating samples. This has been done mainly for consistency when comparing with  $\eta$ , but in any event we do not expect this to affect the diffusion of any but the very largest clusters.

First, we examine the convergence of Eq. (7) by plotting in Fig. 6 the behavior of  $\langle (r_m(t) - r_m(0))^2 \rangle / 6t$  for  $m=1$  (monomers) as a function of time and for three different values of  $p$ . From these curves, we clearly see the existence of long-time tails in the velocity auto-correlation function. Consider the ‘‘Green-Kubo’’ formula corresponding to Eq. (7):

$$\frac{\langle (r_m(t) - r_m(0))^2 \rangle}{t} = \int_0^t ds \langle \mathbf{v}_m(s) \cdot \mathbf{v}_m(0) \rangle (1 - s/t). \quad (8)$$

The dominant contribution to  $\langle (r_m(t) - r_m(0))^2 \rangle / t$  at large times is

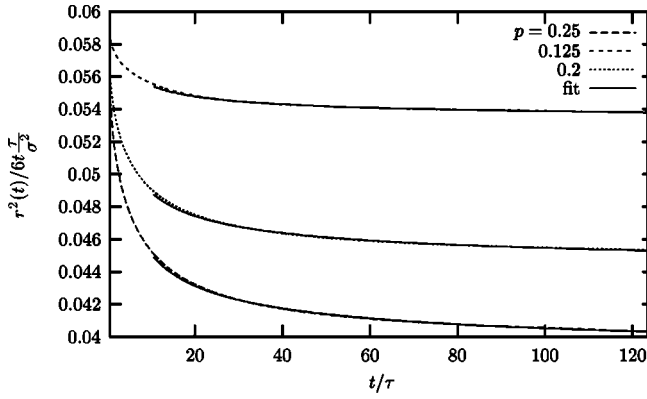


FIG. 6.  $\langle (r_1(t) - r_1(0))^2 \rangle / 6t$  as a function of time for monomers, and for three different values of  $p$ : 0.125, 0.2 and 0.25 from top to bottom. The long-time tails are clearly visible, and the solid lines are fits to the same functional form (see text).

$$\frac{\langle (r_m(t) - r_m(0))^2 \rangle}{t} = D(m, p) - \int_t^\infty ds C_{vv}^{(m)}(s), \quad (9)$$

where  $C_{vv}^{(m)}(s) = \langle \mathbf{v}_m(s) \cdot \mathbf{v}_m(0) \rangle$  is the velocity autocorrelator. Therefore, a power-law tail  $C_{vv}^{(m)}(s) \sim t^{-\alpha}$  in the velocity autocorrelation function will translate into a corresponding power-law tail  $\langle (r_m(t) - r_m(0))^2 \rangle / t \sim D(m, p) + \text{const}(t^{1-\alpha})$  in the Einstein relation. In simple liquids, a value of  $\alpha = 3/2$  is ubiquitous [14], and has also been observed for gelling systems in Ref. [9]; here we find that the same power law provides a very good fit to the data for all  $m$ , but in particular for the small clusters. In Fig. 6, we have also plotted these fits to the power law  $a + bt^{-1/2}$ , and the deviation from the simulation results at early times is barely visible. In Fig. 7, we have done the same for clusters of mass 10, and we see the same behavior. The agreement is slightly worse, presumably due to poorer statistics of larger clusters. We note the existence of a maximum in all of the curves (though not visible in Fig. 6 for  $m=1$ ) for  $\langle (r_m(t) - r_m(0))^2 \rangle / t$ . By differentiating Eq. (8), this can be shown to occur at  $t_m$ , where  $t_m$  is the solution to

$$\int_0^{t_m} ds C_{vv}^{(m)}(s) s = 0. \quad (10)$$

An obvious consequence of the fact that for  $t > t_m$  [using Eq. (9)]

$$\frac{d}{dt} \frac{\langle (r_m(t) - r_m(0))^2 \rangle}{t} \approx C_{vv}^{(m)}(t) < 0 \quad (11)$$

is that  $C_{vv}^{(m)}(t)$  becomes negative (anticorrelation) for large  $t$  and stays negative thereafter. This means that the  $1/\sqrt{t}$  tails in Figs. 6 and 7 correspond to a *negative*  $t^{-3/2}$  tail in  $C_{vv}^{(m)}(t)$ . We also note that  $t_m$  is an increasing function of  $m$  and a decreasing function of  $p$ .

The error made by taking  $D(m, p)$  to be the value of  $\langle (r_m(t) - r_m(0))^2 \rangle / 6t$  at the end of the simulation time  $t = 120\tau$  is negligibly small. For  $p=0.2$ , we have compared

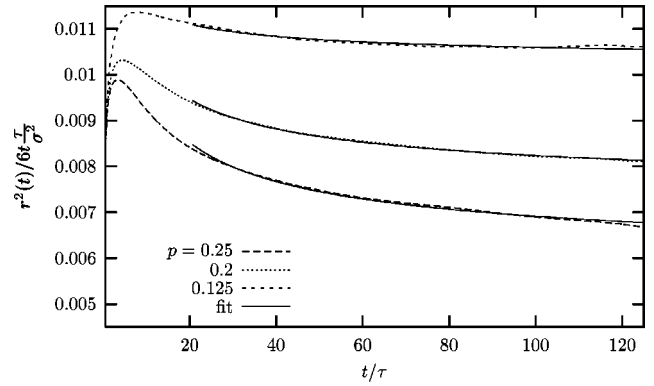


FIG. 7. Same as Fig. 6 but this time for clusters of size 10.

with simulations that are twice as long, and at least for the 20 lightest clusters for which we had good enough statistics, the error was less than 5%. For the smallest  $m$  where the statistics are very good, one can also obtain  $D(m, p)$  from a power-law fit as mentioned above, and the outcome is still consistent with the statement just made (the error here is even much smaller than 5%).

In Ref. [4], we studied  $D(m, p_c)$  and found the power law  $D(m, p_c) \sim m^{-0.69}$ . We have repeated this study up to clusters of size 50 and observe the same behavior over the entire range. For  $p < p_c$ , we see the same power law as a function of  $m$ , at least for small cluster sizes. The quality of the statistics for larger cluster sizes is insufficient to determine whether there is a crossover or cutoff as  $m \rightarrow m^*(p)$ , where  $m^*(p) \sim (p_c - p)^{-1/\sigma}$  is the mass of the largest cluster, but it seems likely that there is. de Gennes has argued that for masses  $1 < m < m^*(p)$ ,  $D(m) \sim m^{-(\nu+s)/(\beta+\gamma)}$  on the basis of a Stokes-Einstein relation with a mass-dependent viscosity [2]. Here  $\beta$  is the exponent that describes the decrease of the order parameter near percolation:  $x_{\text{gel}} \sim (p - p_c)^\beta$ , where  $x_{\text{gel}}$  is the fraction of particles on the spanning cluster and  $p \rightarrow p_c +$ . The other exponents have been introduced already. By using the appropriate scaling relations for 3D percolation [12], the exponent can be rewritten so the prediction is  $D(m) \sim m^{-2(\nu+s)/(d\nu+\gamma)}$ , where  $d=3$  is the Euclidian dimension. With our values for the remaining exponents, we get

$$D(m, p) \sim m^{-0.69} \text{ for } 1 < m < m^*(p). \quad (12)$$

This is in very good agreement with our simulation results within the observed power-law regime. The theoretical prediction can be rewritten as  $D(R_g) \sim R_g^{-(1+s/\nu)}$ , where  $R_g \sim m^{1/D_f}$  is the radius of gyration and  $D_f$  is the fractal dimension. This form of the relation has sometimes (see, for example, Ref. [16]) been used to infer  $s$  from the scaling of  $D$  with  $R_g$ , but to the best of our knowledge the present study presents the first direct verification of such a link.

However, even in this regime one would expect some additional  $p$  dependence of the diffusion coefficient, a point not addressed in Ref. [2]. To this end, we plot in Fig. 8  $D(m, p)$  as a function of  $p$  for monomers, dimers, and trimers, and we see that the diffusion constants decrease (almost

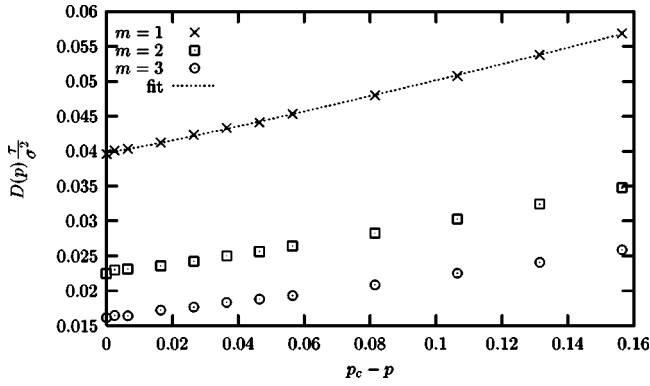


FIG. 8. Diffusion constant as a function of  $p$  for clusters of three different sizes:  $m=1$ ,  $m=2$ , and  $m=3$  from top to bottom. The solid line is a fit to the function  $D(p)=a(p_c-p)^b+D_c$  and  $D_c=0.0398$ ,  $a=0.131$ , and  $b=1.103$  (see text).

linearly) as a function of  $p$ . Moreover, the curves seem to fit nicely to the functional form  $D(p)=a(p_c-p)^b+D_c$ , with a value of the exponent  $b=1.1$ . In Fig. 9, we have made a similar plot for masses  $m=2, \dots, 10$ , and the trends observed above appear to carry over to larger masses. The curves are roughly parallel, and therefore it is not unlikely that the value of  $b$  is independent of  $m$ , but we are unable to confirm this from a fit to the data: the exact value of the exponent appears to be very sensitive to noise in the data.

Finally, we demonstrate a striking violation of the Stokes-Einstein relation when approaching the gelation transition. The idea that  $D \propto 1/\eta$  is used so widely that one may sometimes forget its lack of universal validity. In Fig. 10, however, it is clear that  $D(m,p)\eta$  increases significantly when  $p \rightarrow p_c$ . This is consistent with our previous observations that whereas  $\eta$  diverges at the gelation point,  $D(m,p)$  approaches a nonvanishing constant even for large masses  $m$ . Further away from the gelation point  $p \lesssim 0.20$ , there does, however, seem to be an approximate proportionality between  $D(m,p)$  and  $\eta$ . However, in Figs. 8 and 9 we saw indications that  $D(p) \sim a(p_c-p)^b+D_c$  with  $b > 1$  whereas  $\eta \sim (p_c-p)^{-0.65}$ , and so this apparent proportionality is at best only approximate.

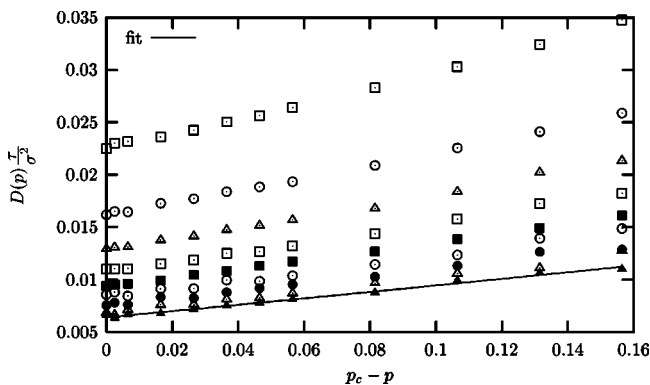


FIG. 9. Same as Fig. 8, but for clusters of sizes  $m=2, \dots, 10$  from top to bottom. The solid line is a fit, and here  $D_c=0.0064$ ,  $a=0.0324$ , and  $b=1.029$ .

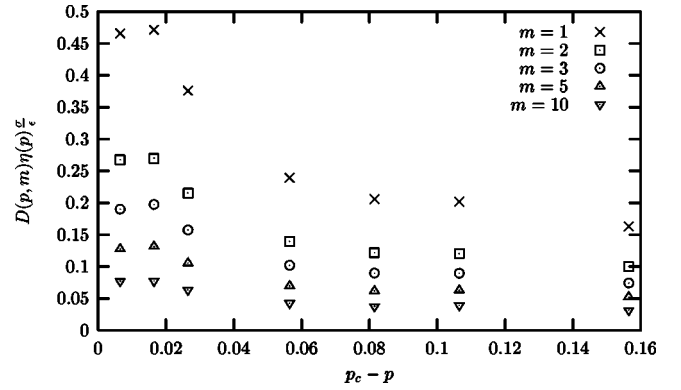


FIG. 10. Plot of  $D(m,p)$  times  $\eta$ ; obviously this is only approximately a constant, as predicted by the Stokes-Einstein relation, far away from  $p_c$ .

## VI. CONCLUSIONS

The main results of this study are the power-law behavior of the mass-dependent diffusion coefficient which seems to hold well away from the critical point, the failure of the Stokes-Einstein relation and the result  $s \approx 0.65$  for the critical exponent of the shear viscosity. This last result, taken together with other recent results [8,9], seems to support the conjecture that the gelation transition is not classifiable in terms of a single universality class: exponents in the range  $0.3 \leq s \leq 0.7$  have been found for models that seem, on the surface, to be very similar. The experimental situation also does not provide much evidence for universality, both exponents near  $s=0.7$  [17–19] and in the range  $1.1 \leq s \leq 1.3$  [20–24] have been reported. We sound a note of caution here: The determination of exponents through finite size scaling is not very precise, especially when quantities that are as difficult to calculate as the shear viscosity form the dataset. However, it seems very unlikely that the errors are large enough that a factor of more than 2 in the exponent could be explained that way.

The mass-dependent diffusion coefficient in this model displays a power-law behavior  $D(m,p) \sim m^{-0.69}$ , consistent with a scaling argument of de Gennes [2]. Reexpressing this in terms of the radius of gyration of clusters through  $m = R_g^{D_f}$ , where  $D_f=2.5$  is the fractal dimension of the percolating cluster, the scaling prediction is  $D(R_g,p) \sim R_g^{-(1+s/\nu)}$ . This yields an estimate  $s=0.65$  for the viscosity exponent, in good agreement with the direct calculation from the Green-Kubo formula. Whether this connection between diffusion and viscosity is general or specific to the present model and whether there exists a similar relationship between diffusion and the elastic shear modulus in the solid phase remains a subject for further study. Using a quite different model, Gado *et al.* [16] have studied the self-diffusion of cross linked polymer clusters on a lattice by bond fluctuation dynamics. They have also used this scaling ansatz to infer the critical exponent of the shear viscosity and found  $s \approx 1.3$ . Their result translates to a mass dependence of the diffusion constant  $D(m,p) \sim m^{-1}$ , very different from that of the present model.

Finally, we have shown that as the fluid becomes more

viscous there is a breakdown of the Stokes-Einstein law  $D\eta \propto k_B T$ , which generally holds for simple liquids. For relatively small concentrations of cross links, this product varies only very little, but for  $p \approx p_c$  the divergence of the viscosity begins to dominate the diffusion constant which seems to saturate for all cluster sizes studied at  $p_c$ .

#### ACKNOWLEDGMENTS

The authors wish to thank B. Jóos and D. Vernon for helpful discussions. Financial support from the Danish National Research Council Grant No. 21-01-0335 and from the NSERC of Canada is gratefully acknowledged.

- 
- [1] M. Adam and D. Lairez, in *Physical Properties of Polymeric Gels*, edited by J.P.C. Addad (Wiley, New York, 1996), p. 87.
  - [2] P. de Gennes, *J. Phys. (France) Lett.* **40**, L197 (1979).
  - [3] K. Broderix, H. Löwe, P. Müller, and A. Zippelius, *Europhys. Lett.* **48**, 421 (1999).
  - [4] S.N. Jespersen, *Phys. Rev. E* **66**, 031502 (2002).
  - [5] M. Küntzel, H. Löwe, P. Müller, and A. Zippelius, e-print cond-mat/0303578.
  - [6] B. Smit, *J. Chem. Phys.* **96**, 8639 (1992).
  - [7] J. Felicity, M. Lodge, and D.M. Heyes, *J. Chem. Soc., Faraday Trans.* **3**, 437 (1997).
  - [8] M. Plischke, B. Jóos, and D. Vernon, *Phys. Rev. E* **67**, 011401 (2003).
  - [9] D. Vernon, M. Plischke, and B. Jóos, *Phys. Rev. E* **64**, 031505 (2001).
  - [10] R.M. Ziff and M.E.J. Newman, *Phys. Rev. E* **66**, 016129 (2002).
  - [11] M.E.J. Newman and R.M. Ziff, *Phys. Rev. E* **64**, 016706 (2001).
  - [12] D. Stauffer and A. Aharony, *Introduction to Percolation Theory*, 2nd ed. (Taylor & Francis, London, 1992).
  - [13] M.P. Allen and D. Tildesley, *Computer Simulation of Liquids* (Oxford Science Publications, Oxford, 1992).
  - [14] J.P. Hansen and I.R. McDonald, *Theory of Simple Liquids* (Academic Press, London, 1976).
  - [15] K. Broderix, T. Aspelmeier, A.K. Hartmann, and A. Zippelius, *Phys. Rev. E* **64**, 021404 (2001).
  - [16] E.D. Gado, L. de Arcangelis, and A. Coniglio, *Eur. Phys. J. E* **2**, 359 (2000).
  - [17] M. Adam, M. Delsanti, D. Durand, G. Hild, and J. Munch, *Pure Appl. Chem.* **53**, 1489 (1981).
  - [18] M. Adam, M. Delsanti, and D. Durand, *Macromolecules* **18**, 2285 (1985).
  - [19] D. Durand, M. Delsanti, and J.M. Luck, *Europhys. Lett.* **3**, 297 (1987).
  - [20] C. Lusignan, T. Mourey, J.C. Wilson, and R.H. Colby, *Phys. Rev. E* **52**, 6271 (1995).
  - [21] J. Martin and J. Wilcoxon, *Phys. Rev. Lett.* **61**, 373 (1988).
  - [22] D. Adolf and J. Martin, *Macromolecules* **23**, 3700 (1990).
  - [23] J. Martin, J. Wilcoxon, and J. Odinek, *Phys. Rev. A* **43**, 858 (1991).
  - [24] J. Martin, J. Wilcoxon, and D. Adolf, *Phys. Rev. Lett.* **61**, 2620 (1988).